Higher Surface Energy of Free Nanoparticles

K. K. Nanda,[1,*] A. Maisels,[1] F. E. Kruis,[1] H. Fissan,[1] and S. Stappert[2]

[1]*Department of Electrical Engineering and Information Technology, University Duisburg-Essen, 47048 Duisburg, Germany*
[2]*Experimental Physics, University Duisburg-Essen, 47048 Duisburg, Germany*

(Received 18 February 2003; published 4 September 2003)

We present an accurate online method for the study of size-dependent evaporation of free nanoparticles allowing us to detect a size change of 0.1 nm. This method is applied to Ag nanoparticles. The linear relation between the onset temperature of evaporation and the inverse of the particle size verifies the Kelvin effect and predicts a surface energy of 7.2 J/m^2 for free Ag nanoparticles. The surface energy of nanoparticles is significantly higher as compared to that of the bulk and is essential for processes such as melting, coalescence, evaporation, growth, etc., of nanoparticles.

DOI: 10.1103/PhysRevLett.91.106102 PACS numbers: 68.60.Dv, 68.35.Md

Based on thermodynamic arguments, Tolman [1] predicted that the surface energy should decrease with decreasing particle size. This tendency follows from the assumption that the Tolman length δ is positive. However, δ is predicted to be negative by a rigorous thermodynamic derivation [2], which would lead to an increase of the surface energy with decreasing size. In addition to the uncertainty in the sign of δ, the validity of the Tolman equation is questionable for very small particles [3]. Further, the absolute value [1] of δ is in the subnanometer (10^{-10} m) range; the effect of size on the surface energy is important when the size is comparable with that of an atom. For nanoparticles, larger values of surface energy as compared to the bulk material have been reported from the size-dependent lattice parameter (SDLP) [4–12]. For example, the surface energy of Pd nanoparticles in a polymer matrix [10] has been found to be 6.0 ± 0.9 J/m^2, whereas that of the bulk is 1.808 J/m^2. Similarly, the surface energy of capped and bare CdS nanoparticles [11] has been found to be 1.74 and 2.50 J/m^2, respectively, whereas that of bulk CdS is 0.75 J/m^2. In some cases, the compressibility (κ) increases with decreasing particle size as observed for PbS nanoparticles [13]. If this is the case, one would obviously end up with a higher value of surface energy as the compressibility is assumed to be constant when it is estimated from SDLP of nanoparticles. In case of CdS, a higher value has been obtained although the compressibility of CdS nanoparticles is the same as that of the bulk [11].

In a recent Letter [14], a linear relation has been obtained between the evaporation temperature and the inverse of the particle size for free PbS nanoparticles that verifies the Kelvin effect [15] and allows us to estimate the surface energy of nanoparticles. A constant value of 2.45 J/m^2 is found for the surface energy of PbS nanoparticles [14]. The only report on the surface energy of bulk PbS delivers a value of 0.0383 J/m^2 [16], which is much smaller when compared with that of PbS nanoparticles (2.45 J/m^2) and other ionic semiconductors (~ 1 J/m^2). On the other hand, a value of 1.4 J/m^2 has been calculated for bulk PbS by using the empirical equation [17]. Since the data on the surface energy of bulk PbS seem to be ambiguous, the higher surface energy of nanoparticles should be verified for other systems.

Silver is one of the most widely studied materials, and there is a wide range of values reported for the surface energy. The value obtained from SDLP of nearly free Ag nanoparticles is $\sim$6.4 J/m^2 [4–6], that of embedded Ag nanoparticles is in the range 1.3–5.9 J/m^2 [6–9], whereas that of bulk is in the range 1.065–1.54 J/m^2. The different values of surface energy clearly indicate its dependency on the surrounding matrix as well as on the particle-substrate interaction. Furthermore, it has been reported that the surface energy of Ag deduced from the size dependency of a_{111} and a_{220} lattice constants is 6.405 and 1.415 J/m^2, respectively [5]. Hofmeister *et al.* [6] have also obtained a surface energy of 6.3 J/m^2 from the size dependency of a_{111}. However, the highest [18] value of the surface energy of Ag in (111) and (110) directions as predicted by a "universal bonding relation" [19] is 1.27 and 1.54 J/m^2, respectively. This suggests that the discrepancy between the surface energies as determined from different lattice constants [5] may be due to the anisotropy in κ. The surface energy is the only free parameter in the Kelvin equation [14] and there is no such ambiguity in evaluating the surface energy from the size-dependent evaporation of nanoparticles. Blackman *et al.* [20] studied the time taken for the complete evaporation of Ag nanoparticles on a carbon substrate by maintaining a constant sample temperature and obtained a surface energy of 1.13 J/m^2 by comparing the data with the Kelvin equation. This value of the surface energy is in excellent agreement with that of bulk Ag but lower as compared to that obtained for nearly free Ag nanoparticles. The above discussions indicate that Ag is an ideal material for the study of size-dependent evaporation so that the validity of the Kelvin equation can be tested and the surface energy obtained from this method can be compared. In this Letter, the size-dependent evaporation of free Ag nanoparticles is investigated by online heat

treatment of size-classified aerosols at different temperatures for a particular time period. The linear relation between the evaporation temperature and the inverse of the particle size verifies the Kelvin effect as is the case of PbS [14]. From the slope, a constant value of 7.2 J/m^2 is obtained for the surface energy of free Ag nanoparticles which is in excellent agreement with that obtained from SDLP but higher as compared to that of bulk. It is one of the important physical quantities that controls the growth of a material on a substrate as well as different phenomena such as melting, coalescence, evaporation, phase transition, growth, etc., of nanoparticles and is essential to be known.

The experimental setup is similar to that employed in Ref. [14]. In brief, a Ag aerosol is formed by evaporating Ag flakes in a tube furnace at a temperature of 1398 K under nitrogen atmosphere and subsequent cooling down of the vapor. In order to size classify the agglomerates/particles, they are charged by a radioactive β source (^{85}Kr), and flown into a differential mobility analyzer (DMA). A DMA selects particles on the basis of their electrical mobility which is a function of their size, charge level, and shape. The mobility-equivalent diameter d_M is equal to the geometric diameter for spherical, singly charged particles. After size classification, a second tube furnace is used to investigate the evaporation of Ag nanoparticles. The residence time of the agglomerates/nanoparticles in this furnace is $\sim$35 s when the flow of the carrier gas is 1.0 standard liters per minute (slm). In Ref. [14], the particle sizes at different sintering temperatures have been determined by a transmission electron microscope (TEM) and a fitting procedure has been employed to determine the onset temperature of evaporation. In this study, a tandem DMA technique [21,22], i.e., a second DMA is used after the sintering furnace to detect the change in the mobility-equivalent diameter. The DMA can detect a change of 0.1 nm in the mobility-equivalent diameter, whereas it is very difficult to detect such a small change by TEM. The method employed here is more effective, fast and accurate as compared to the method described in Ref. [14].

Figure 1(a) shows the change in the particle size distributions at the outlet of the sintering furnace against the mobility-equivalent diameter. The mobility-equivalent diameter of the maximum of the particle concentration is considered as the representative particle size at the outlet of the sintering furnace. The mobility-equivalent diameter d_M of Ag nanoparticles with different initial mobility diameters d_{M0} as a function of the sintering temperature is shown in Fig. 1(b). It can be noted that the mobility diameter first decreases with increasing sintering temperature, enters a flat regime, and then decreases when the sintering temperature is increased further. The first decrease in the mobility-equivalent diameter is associated with the compaction of the agglomerates/particles. This compaction occurs at a temperature of 423 $\pm$ 20 K

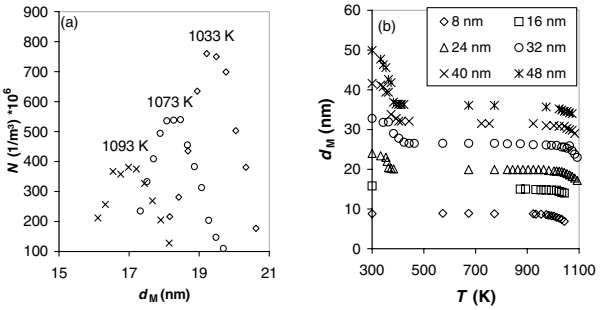

FIG. 1. (a) Size distributions of Ag nanoparticles as measured by a DMA at the outlet of the sintering furnace. The initial mobility-equivalent diameter d_{M0} as selected by a DMA is 24.0 nm. (b) d_M as a function of the sintering temperature for different values of d_{M0}.

which is lower than the temperature predicted for the coalescence of three Ag clusters of 309 atoms each by molecular dynamic (MD) simulations [23]. The discrepancy between the experiments and the MD simulations may be due to the difference in the time scale [24]. As a consequence of the compaction, the surface area and, hence, the mobility-equivalent diameter decrease until the agglomerates are fully sintered to yield compact particles, and one obtains the flat regime. When the sintering temperature is increased further, the particle size decreases due to partial evaporation and, hence, the mobility-equivalent diameter decreases. Figure 1(b) clearly indicates that the temperature at which the particle size decreases due to evaporation of Ag nanoparticles depends on the initial mobility diameter.

Before we evaluate the size-dependent evaporation of Ag nanoparticles from Fig. 1, it is essential to compare the mobility-equivalent diameter with the geometric diameter for spherical particles. TEM micrographs (taken on a Philips CM12 twin microscope, 120 keV, LaB6 cathode) for particles with initial mobility-equivalent diameter of 16.0 nm sintered at 913, 933, 1023, and 1043 K are presented in Fig. 2. It can be noted that the mobility-equivalent diameter is consistent with the size determined from the TEM for a sintering temperature of 1023 and 1043 K. As the mobility-equivalent diameter is equal to the geometric diameter of the spherical particle, it is concluded that the particles sintered at 1023 and 1043 K are spherical and the particle size measured by the DMA is sufficiently precise for the analysis. The deviation of about 1.0 nm between d_M and particle diameters according to TEM for sintering temperatures of 913 and 933 K is due to the particle nonsphericity. Here, the particle geometry is expected to be an ellipsoid (aspect ratio less than but close to unity) as predicted by the MD simulations of coalesced particles [23].

To determine the onset temperature of evaporation, the data of Fig. 1 are plotted as the reduced mobility-equivalent diameter d_M/d_{M0} versus the sintering temperature as shown in Fig. 3(a). An interpolation procedure

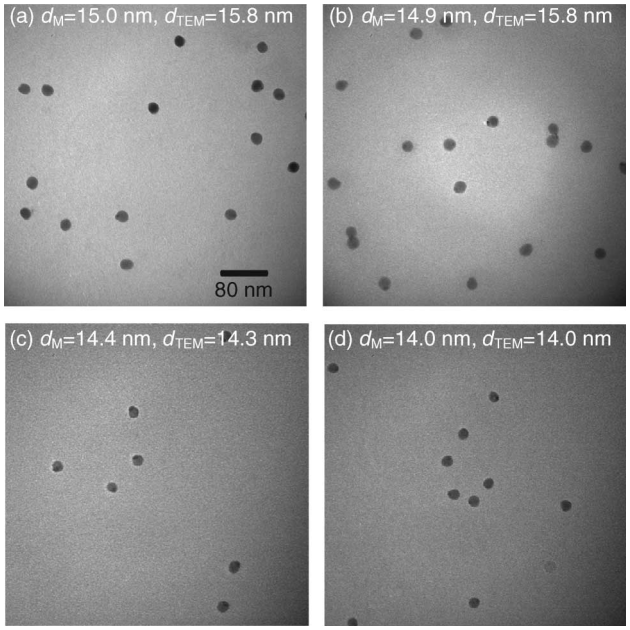

FIG. 2. TEM micrographs of Ag agglomerates/nanoparticles sintered at different temperatures ($d_{M0} = 16.0$ nm). The micrographs (a)–(d) correspond to sintering temperatures of 913, 933, 1023, and 1043 K.

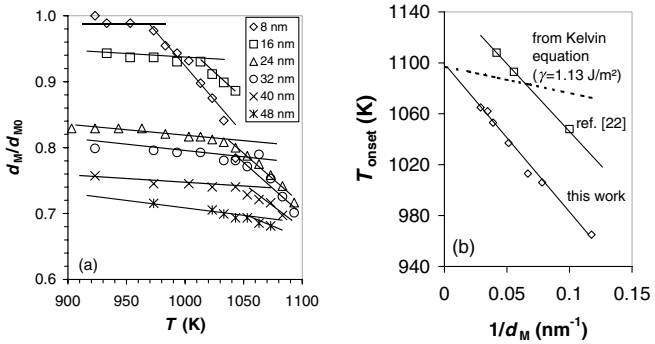

FIG. 3. (a) The reduced mobility-equivalent diameter as a function of the sintering temperature. The particle size and the onset temperature of evaporation are obtained by an interpolation technique shown in the figure. (b) The onset temperature of evaporation versus the inverse of particle size.

is adopted to obtain the particle size and the onset temperature of evaporation (T_{onset}), as demonstrated in the figure. Then, T_{onset} is plotted against the inverse of the particle size as shown in Fig. 3(b) indicating a linear relation between them which verifies the Kelvin effect. The solid line is a least-squares fit to the experimental data yielding a slope of 1158 ± 55 nm K and an intercept of 1097 ± 4 K, the latter representing a temperature where large particles evaporate. Data extracted from the measurements of Shimada *et al.* [22] are also plotted for comparison. The higher evaporation temperature with nearly the same slope may be due to a different residence time [14].

To extract the surface energy of free Ag nanoparticles, the size-dependent evaporation data are analyzed based on the Kelvin equation. The vapor pressure (p_s) of nanoparticles is related to that of a flat surface (p_{s0}) as [15]

$$\frac{p_s}{p_{s0}} = \exp\left(\frac{4\gamma M}{\rho_p RTd}\right), \tag{1}$$

where γ is the surface energy, M is the molecular weight, ρ_p is the density of the particle, R is the gas constant, T is the temperature, and d is the particle size. For the bulk vapor pressure (p_{s0}) of Ag, we use the expression

$$\log p_{s0}(\text{Torr}) = -1.526 \times 10^4 \frac{1}{T(\text{K})} - 6.649 \times 10^{-4} T(\text{K}) + 10.62, \tag{2}$$

which is obtained by fitting the vapor pressure data in the temperature range of 895–1100 K [25]. As the evaporation of large particles is expected to take place at 1097 K and the influence of the Kelvin effect can easily be neglected for large particles, the vapor pressure of Ag at this temperature is calculated to be 9.59×10^{-5} Torr. Using the procedure as described in Ref. [14], a surface energy of 7.20 and 6.82 J/m^2 is found from our experimental data and the data of Shimada *et al.* [22] for free Ag nanoparticles. These values are consistent and in excellent agreement with that obtained for nearly free Ag particles from SDLP [6–9]. In contrast, a surface energy of 1.13 J/m^2 has been obtained by Blackman *et al.* [20] for Ag nanoparticles on a carbon substrate. Assuming a surface energy of 1.13 J/m^2 for Ag nanoparticles [20], the size-dependent evaporation temperature is evaluated and presented in Fig. 3(b) as a dashed line for comparison. A stronger size dependency of the evaporation temperature for free nanoparticles is noteworthy and yields a higher surface energy. In this context, it may be noted that the Tolman equation cannot explain the high value of the surface energy for Ag nanoparticles as the particle size has only a weak influence on the surface energy in the size range studied.

In the bulk, atoms are evenly surrounded and the cohesive forces between the atoms tend to balance. However, there are atoms on only one side of the free nanoparticle surface, and there is a net inward cohesive force. As the particle size decreases, the net inward cohesive force increases, and as a consequence the surface energy that depends on the net inward cohesive force should increase with decreasing particle size. If the nanoparticles are capped or embedded in a matrix, the net inward force reduces, thereby reducing the surface energy. The size dependency of the cohesive energy is also expected to influence the evaporation temperature. The activation energy E_A (N) needed to remove one atom from a nanoparticle is related to bulk cohesive energy per atom (E_B) as [26]

$$E_A(N) = E_B - \frac{8\pi}{3} r_s^2 \gamma N^{-1/3}, \quad (3)$$

where r_s is the radius of a sphere corresponding to the volume of one atom in bulk and N is the number of atoms in the nanoparticles related to the particle radius as $R = r_s N^{1/3}$. By scaling the activation energy to the onset temperature of evaporation, Eq. (4) can be expressed as

$$\frac{T_{\text{onset}}}{T_{\text{onset},b}} = 1 - \frac{16\pi\gamma r_s^3}{3E_B d}, \quad (4)$$

where $T_{\text{onset},b}$ represents the evaporation temperature of the bulk. Equation (4) also predicts a linear relation between T_{onset} and the inverse of the particle size, and the slope depends on the surface energy of the nanoparticles. Using $E_B = 2.95$ eV and $r_s = 0.158$ nm in Eq. (4), a surface energy of 7.37 J/m^2 is obtained by analyzing our experimental data of Ag. It is possible that both the Kelvin equation and Eq. (4) contribute to the stronger size-dependent evaporation of free nanoparticles and a higher surface energy is obtained when the experimental data are compared with one of the theoretical predictions. As the Kelvin effect and Eq. (4) contribute equally to the size-dependent evaporation of nanoparticles, the surface energy of nanoparticles were expected to be twice that of the bulk. However, the surface energy of Ag nanoparticles is 5–6 times higher than that of the bulk, which infers that the higher surface energy is an intrinsic property of nanoparticles. This observation is well supported by the MD simulations of Rytkönen *et al.* [26]. They obtained a surface energy of 41.6 mJ/m^2 from the binding energies of icosahedral argon clusters, whereas that of the bulk is 23 mJ/m^2. Although the interaction potential of Ag atoms is not that of Ar atoms, one may expect that the MD simulations can shed some light on the higher surface energy of Ag nanoparticles. The similarity of variations of the size-dependent melting temperature calculated by MD simulations for Ar [26] and Ag [23] clusters justifies this expectation.

In summary, an accurate and fast method to study the size-dependent evaporation of nanoparticles has been reported. This method is applied to Ag nanoparticles that verifies the Kelvin effect and allows one to determine the surface energy. A constant surface energy of 7.2 J/m^2 has been obtained for Ag nanoparticles in the size range studied, which is in excellent agreement with that obtained from the SDLP of nearly free Ag nanoparticles but higher as compared to that of bulk. This also demonstrates that the surface energy of free nanoparticles is higher as compared to that of embedded nanoparticles. The surface energy is expected to be higher for all systems which is in contrast with Tolman's prediction and poses a challenge to understand it. All the physical processes as well as the physical parameters of nanoparticles that depend on the surface energy will be modified.

This work is financially supported by Deutsche Forschungsgemeinschaft (DFG) in the framework of the special research program "Nanoparticles from the gas phase: formation, structure, properties" (SFB 445, Projects No. A7 and No. B1) and priority program "Handling of highly dispersed powders" (SPP 1062).

*Email address: nanda@uni-duisburg.de

[1] R. C. Tolman, J. Chem. Phys. **17**, 333 (1949).
[2] E. v. Giessen, E. M. Blokhuis, and D. J. Bukman, J. Chem. Phys. **108**, 1148 (1998).
[3] K. Koga, X. C. Zeng, and A. K. Shchekin, J. Chem. Phys. **109**, 4063 (1998).
[4] C. R. Berry, Phys. Rev. **88**, 596 (1952).
[5] H. J. Wasserman and J. S. Vermaak, Surf. Sci. **22**, 164 (1970).
[6] H. Hofmeister, S. Thiel, M. Dubiel, and E. Schurig, Appl. Phys. Lett. **70**, 1694 (1997).
[7] M. Dubiel, H. Hofmeister, and E. Schurig, Phys. Status Solidi (b) **203**, R5 (1997).
[8] P. A. Montano *et al.*, Phys. Rev. B **30**, 672 (1984).
[9] T. de Planta, R. Ghez, and F. Piuz, Helv. Phys. Acta **37**, 74 (1964).
[10] R. Lamber, S. Wetjen, and N. I. Jaeger, Phys. Rev. B **51**, 10 968 (1995).
[11] A. N. Goldstein, C. M. Echer, and A. P. Alivisatos, Science **256**, 1425 (1992).
[12] C. Solliard and M. Flueli, Surf. Sci. **156**, 487 (1985).
[13] S. B. Qadri *et al.*, Appl. Phys. Lett. **69**, 2205 (1996).
[14] K. K. Nanda, F. E. Kruis, and H. Fissan, Phys. Rev. Lett. **89**, 256103 (2002).
[15] W. Thomson (Kelvin), Philos. Mag. **42**, 448 (1871).
[16] B. Janczuk *et al.*, Mater. Chem. Phys. **37**, 64 (1994).
[17] K. K. Nanda, S. N. Sahu, and S. N. Behera, Phys. Rev. A **66**, 13 208 (2002).
[18] M. Methfessel, D. Hennig, and M. Scheffler, Phys. Rev. B **46**, 4816 (1992).
[19] J. R. Smith and A. Banerjea, Phys. Rev. Lett. **59** , 2451 (1987).
[20] M. Blackman, N. D. Lisgarten, and L. M. Skimmer, Nature (London) **217**, 1245 (1968).
[21] D. J. Rader and P. H. McMurry, J. Aerosol Sci. **17**, 771 (1986).
[22] M. Shimada, T. Seto, and K. Okuyama, AIChE J. **39**, 1859 (1993).
[23] S. J. Zhao, S. Q. Wang, Z. Q. Yang, and H. Q. Ye, J. Phys. Condens. Matter **13**, 8061 (2001).
[24] K. E. J. Lehtinen and M. R. Zachariah, Phys. Rev. B **63**, 205402 (2001).
[25] R. A. Honig and D. A. Kramer, RCA Rev. **30**, 285 (1969).
[26] A. Rytkönen, S. Valkealahti, and M. Manninen, J. Chem. Phys. **106**, 1888 (1997).